Structure and Conformation of Spin-Labeled Methyl L-Phenylalanate and L-Phenylalanine Determined by Electron Nuclear Double Resonance Spectroscopy[1a]

Heikki Joela,[1b] Devkumar Mustafi, C. Christine Fair, and Marvin W. Makinen*

Department of Biochemistry and Molecular Biology, The University of Chicago, Cummings Life Science Center, 920 E. 58th Street, Chicago, Illinois 60637 *(Received: April 23, 1991; In Final Form: June 20, 1991)*

The conformation of L-phenylalanine and of methyl L-phenylalanate acylated at the amino nitrogen position with the nitroxyl spin-label 2,2,5,5-tetramethyl-1-oxypyrroline-3-carboxylic acid has been determined by electron nuclear double resonance (ENDOR) spectroscopy and molecular modeling. ENDOR resonance absorptions of spin-labeled derivatives in frozen glassy solutions were well resolved for each class of protons of the amino acid moiety under conditions of low modulation depth of the radio-frequency field and were assigned by selective deuteration. From the maximum and minimum ENDOR shifts that corresponded to the principal hyperfine coupling components, the dipolar hyperfine contributions were calculated to estimate electron-nucleus separations. Spin-labeled derivatives of L-phenylalanine with fluorine substituted at the $C^{\delta 1}$- and C^{ζ}-positions of the side chain were employed for assigning the conformation of the aromatic side chain. Conformational analysis on the basis of torsional angle search calculations constrained by the ENDOR determined electron-nucleus separations showed that the predominant conformer of spin-labeled derivatives of the $C^{\delta 1}$-fluorinated derivatives of L-phenylalanine and of its methyl ester analogue belongs to the classical g^- rotamer in which the $[C^{\alpha}-C^{\beta}-C^{\gamma}-C^{\delta 1}(-F)]$ torsion angle has a value of $-83°$ corresponding to an antiperpendicular orientation of the *o*-fluorobenzyl side chain. The results are explained on the basis of dipolar interactions between the peptide bond, the carboxylate group, and the *o*-fluorobenzyl side chain. This conformation of the side chain was independent of solvent polarity. The results also indicate that in the preferred conformer the carboxylate group acquires a conformation similar to that of a fully extended polypeptide in a β-strand.

Introduction

In general, the conformational properties of the aromatic side chains in amino acids and in peptides in solution are poorly defined. Although peptide and amino acid conformation has been investigated by application of nuclear magnetic resonance (NMR[2]) methods, structural assignments depend on estimates of vicinal, through-bond coupling constants to calculate the values of dihedral angles and on the chemical shift of the $-C^{\beta}H_2-$ protons to assess the fractional populations of the various rotamers present.[3-5] While the value of the χ_1 dihedral angle of the side chain measuring rotation around the $C^{\alpha}-C^{\beta}$ bond can be generally estimated on the basis of NMR data, it is not always feasible to assign the value of the dihedral angle χ_2 for rotation about the $C^{\beta}-C^{\gamma}$ bond because it is often difficult to assign the resonances due to the $-C^{\beta}H_2-$ group of the side chain of aromatic amino acids.[5] The most detailed knowledge of the conformational properties of peptides and other derivatives of amino acids is, thus, necessarily obtained through structure determination by X-ray crystallographic methods. This approach, while extremely important in structural chemistry, does not allow ready application to a number of important problems in biochemistry.

It has been appreciated for some time that methods of three-dimensional structure analysis coupled with application of cryoenzymology can provide a means to characterize the molecular structures of true intermediates of enzyme-catalyzed reactions.[6] However, under the conditions of fluid organic-aqueous cosolvent mixtures of high viscosity at subzero temperatures, the efficacy of application of NMR and X-ray diffraction methods for such problems becomes extremely limited because of both technical limitations and the finite, intrinsic, albeit lengthened, lifetime of a reaction intermediate accumulated in a fluid cryosolvent mixture. In this laboratory, we have endeavored to develop a method of three-dimensional structure determination and conformational analysis that can be applied to low-temperature stabilized enzyme reaction intermediates in frozen (glassy) solutions. To this end we have shown that electron nuclear double resonance (ENDOR[2]) spectroscopy, particularly of nitroxyl spin-labeled molecules, can be incisively applied to determine structure and conformation of molecules in frozen solutions or polycrystalline states with an accuracy that is exceeded only by that of single-crystal X-ray diffraction methods.[7,8]

In this publication we have determined the conformational properties of L-phenylalanine and its methyl ester acylated at the amino nitrogen position with the spin-label 2,2,5,5-tetramethyl-1-oxypyrroline-3-carboxylic acid by using ENDOR spectroscopy. With use of spin-labeled phenylalanine containing *o*- or *p*-fluorine substituents on the benzyl side chain, we demonstrate how rotamer structure can be assigned. We show also that the interaction of the electric (ground state) dipole of an ortho-fluorinated benzyl side chain with the amide and ester linkages in the molecule is the determinant of its conformation. Together with our earlier study of spin-labeled methyl L-tryptophanate,[8b] the results provide an unusually accurate basis for structure definition of amino acid derivatives that can be employed as substrates of proteolytic enzymes. Subsequent publications[9] will be directed toward characterization by ENDOR of the conformation of these spin-labeled amino acids as substrates in low-temperature-stabilized intermediates of enzyme reactions.

Experimental Procedures

General Materials. Carbonyl-1,1'-diimidazole, L-phenylalanine, D,L-δ-fluorophenylalanine (99%), and D,L-ζ-fluorophenylalanine (>97%) were obtained from Aldrich Chemical Co. Inc. (Milwaukee, WI). Specifically labeled L-(α-^{2}H)- (95%), L-(δ1,δ2,ϵ1,ϵ2,ζ-$^2H_5$)- (98.7%), L-(β1,β2,δ1,δ2,ϵ1,ϵ2,ζ-$^2H_7$)- (98.7%),

(1) (a) This work was supported by grants of the National Institutes of Health (AA 06374 and GM 21900) and the National Science Foundation (BBS 8616566). (b) Permanent address: Department of Chemistry, University of Jyväskylä, SF-40100 Jyväskylä, Finland. Supported in part by the E. Aaltonen Foundation.

(2) Abbreviations: DMSO, dimethyl sulfoxide; ENDOR, electron nuclear double resonance; EPR, electron paramagnetic resonance; hf, hyperfine; hfc, hyperfine coupling; NMR, nuclear magnetic resonance; THF, tetrahydrofuran.

(3) (a) Feeney, J. *Proc. R. Soc. London, A* **1975**, *345*, 61. (b) Wüthrich, K. *NMR of Proteins and Nucleic Acids*; Wiley: New York, 1986.

(4) (a) Dezube, B.; Dobson, C. M.; Teague, C. E. *J. Chem. Soc., Perkin Trans. 2* **1981**, 730. (b) Levine, B. A.; Williams, R. J. P. *Proc. R. Soc. London, A* **1975**, *345*, 5.

(5) (a) Reddy, M. C.; Nagi Reddy, B. P.; Sridharan, K. R.; Ramakrisna, J. *Org. Magn. Reson.* **1984**, *22*, 464. (b) Mikhova, B. P.; Simenov, M. F.; Spassov, S. L. *Magn. Reson. Chem.* **1985**, *23*, 474. (c) Reddy, M. C.; Nagi Reddy, B. P.; Ramakrishna, J. *Indian J. Biochem. Biophys.* **1986**, *23*, 286.

(6) (a) Makinen, M. W.; Fink, A. L. *Annu. Rev. Biophys. Bioeng.* **1977**, *6*, 301. (b) Cartwright, S. J.; Fink, A. L. *CRC Crit. Rev. Biochem.* **1981**, *11*, 145.

(7) Wells, G. B.; Makinen, M. W. *J. Am. Chem. Soc.* **1988**, *110*, 6343.

(8) (a) Mustafi, D.; Sachleben, J. R.; Wells, G. B.; Makinen, M. W. *J. Am. Chem. Soc.* **1990**, *112*, 2558. (b) Wells, G. B.; Mustafi, D.; Makinen, M. W. *J. Am. Chem. Soc.* **1990**, *112*, 2566.

(9) Wells, G. B.; Mustafi, D.; Makinen, M. W., manuscript in preparation.

0022-3654/91/2095-9135$02.50/0

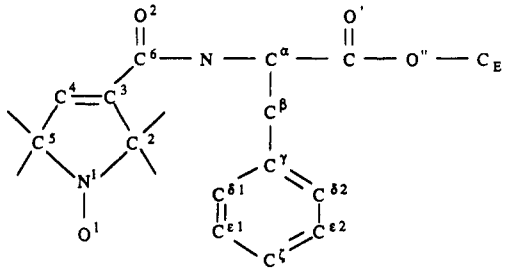

I. SL methyl *L*-phenylalanate

II. SL methyl *L*-(α-^{2}H)-phenylalanate

III. SL ($^2H_3$)methyl *L*-(δ1, δ2, ε1, ε2, ζ-$^2H_5$)-phenylalanate

IV. SL ($^2H_3$)methyl *L*-(β1, β2, δ1, δ2, ε1, ε2, ζ-$^2H_7$)-phenylalanate

V. SL methyl *L*-(α, β1, β2, δ1, δ2, ε1, ε2, ζ-$^2H_8$)-phenylalanate

VI. SL methyl *D, L*-(δ-F)-phenylalanate

VII. SL methyl *D, L*-(ζ-F)-phenylalanate

Figure 1. Illustration of the chemical bonding structure and the atomic numbering scheme of specifically fluorinated and deuterated analogues of methyl *N*-(2,2,5,5-tetramethyl-1-oxypyrrolinyl-3-carboxyl)phenylalanate employed in this study. SL refers to the spin-label acyl moiety attached to the amino nitrogen atom. In the text, compounds designated by primed Roman numerals are the corresponding carboxylic acid analogues of phenylalanine.

and L-(α,β$_1$,β$_2$,δ1,δ2,ε1,ε2,ζ-$^2H_8$)-phenylalanine (98.6%) were obtained from MSD Isotopes (St. Louis, MO). Deuterated solvents and reagents were obtained from Cambridge Isotope Laboratories, Inc. (Woburn, MA) or Aldrich Chemical Co. The spin-label 2,2,5,5-tetramethyl-1-oxypyrroline-3-carboxylic acid was obtained by hydrolysis of the corresponding carboxamide (Molecular Probes, Eugene, OR) as described by Rosantzev.[10] All other reagents were used as previously described.[8]

Methyl L-Phenylalanate Hydrochloride. The methyl ester of L-phenylalanine was prepared in over 90% yield as earlier described for L-alanine and L-tryptophan with use of doubly distilled, colorless thionyl chloride.[8] Mass spectra of the product multiply recrystallized from methanol/methyl acetate (mp 160.5–161.5 °C) showed that the highest molecular ion peak corresponded to an [M$^+$] species of molecular weight 180, indicating that this species is the protonated methyl phenylalanate ester. Specifically deuterated derivatives yielded analogous results with identical melting points. Methyl esters of the fluorinated analogues were similarly synthesized and crystallized from methanol/methyl acetate with mp of 178–179.5 and 156.5–157.5 °C for the D,L-ζ-fluoro- and D,L-δ-fluorophenylalanine isomers, respectively.

Methyl *N*-(2,2,5,5-Tetramethyl-1-oxypyrrolinyl-3-carbonyl)-L-phenylalanate. The series of natural-abundance and specifically deuterated and fluorinated analogues of spin-labeled methyl L-phenylalanate employed in this investigation is illustrated in Figure 1. The synthesis procedure for I–VII essentially followed that described earlier for spin-labeled derivatives of methyl L-alanate and methyl L-tryptophanate.[8] The oily product was recrystallized from diethyl ether/pentane (60:40 v/v), generally with greater than 25% yield. Typical results for elemental analysis of the yellow, multiply recrystallized products showed the following (calcd/exptl): C, 66.07/66.09; H, 7.30;7.46; N, 8.11/8.04 for I (mp 70.5–73.0 °C); C, 64.56/63.89; H, 7.13/7.06; N, 7.92/8.26 for III (mp 67.0–69.0 °C); C, 62.63/61.74; H, 6.64/6.70; N, 7.69/7.52; F, 5.21/5.38 for VI (mp 87.0–88.0 °C). Mass spectra of I showed the highest molecular ion peak to correspond to the expected *m/e* ratio of 345 with the characteristic breakdown pattern of oxypyrrolinyl spin-label species.[11] The mass spectra of other specifically deuterated and fluorinated analogues gave comparable results.

N-(2,2,5,5-Tetramethyl-1-oxypyrrolinyl-3-carbonyl)-L-phenylalanine. We describe the general procedure for deuterated analogues because of the need to optimize the yield for expensive specifically deuterated starting materials.

For a typical synthesis of III′, for instance, the acid chloride of 2,2,5,5-tetramethyl-1-oxypyrrolinyl-carboxylic acid was prepared from 0.33 g (1.79 mmol) of the carboxylic acid derivative suspended in 3 mL of benzene freshly distilled and dried over sodium metal, as previously described.[10,12] The oily product was dissolved in 1.5 mL of freshly distilled tetrahydrofuran (THF) and added dropwise over 30 min to a solution of L-(δ1,δ2,ε1,ε2,ζ-$^2H_5$)-phenylalanine (0.30 g, 1.79 mmol) in 10 mL of water buffered to pH > 10 with 0.25 M sodium carbonate and 0.25 M sodium hydroxide at 0 °C. The pH was adjusted as necessary with 1 N NaOH during addition of the acid chloride, and the reaction mixture was stirred overnight at room temperature. The reaction mixture was then adjusted to pH 5.5 by dropwise addition of 2 N HCl under vigorous stirring, followed by extraction with methylene chloride. Further acidification of the aqueous layer to pH 3.5 produced a light yellow precipitate. This was taken up in methylene chloride, and the organic solution was then dried over anhydrous sodium sulfate. Removal of solvent in vacuo produced the yellow product, which was crystallized (mp 160.5–161.5 °C) from THF/pentane in greater than 50% yield. Elemental analysis showed the following (calcd/exptl): C, 65.24/64.98; H, 7.00/6.99; N, 8.45/8.39 for I′; and C, 64.26/63.98; H, 6.89/7.04; N, 8.33/8.23, for III′. Mass spectra showed the highest molecular ion peak to correspond to the expected *m/e* ratios of 331 for I′ and 336 for III′. Syntheses of other specifically deuterated and fluorinated analogues produced comparable results.

EPR and ENDOR. ENDOR spectra were recorded with the sample at 20 K with an X-band Bruker ER200D spectrometer equipped with an Oxford Instruments ESR10 liquid helium cryostat and a Bruker digital ENDOR accessory, as previously described.[8,13] ENDOR spectra were recorded in the first-derivative absorption mode under typical conditions of approximately 0.6 mW of incident microwave power, 12.5-kHz frequency modulation, 50 W rf power, and 7–9-kHz modulation depth of the rf field. We have previously estimated that under these conditions for the cylindrical Bruker ENDOR cavity $H_1 \sim 0.04$ G and $H_2 \sim 1.5$ G in the rotating frame.[13b] The static laboratory field was not modulated for ENDOR. Spin-labeled derivatives were dissolved to a concentration of 5×10^{-3} M in ($^2H_4$)methanol, 50:50 (v/v) (^{2}H)chloroform:($^2H_8$)toluene, or 10:45:45 (v/v) ($^2H_6$)dimethyl sulfoxide:(^{2}H)chloroform:($^2H_8$)toluene.

ENDOR spectra were collected under conditions of two different settings of the static laboratory magnetic field: setting A corresponding to microwave power saturation of the low-field EPR absorption feature of nitroxyl spin-labels, and setting B corresponding to microwave power saturation of the central EPR absorption feature of spin-labels, as described in earlier studies from this laboratory.[7,8] ENDOR line widths were evaluated as the line width at half-maximum intensity for parallel absorption features and as the peak-to-peak line width for perpendicular absorption features. We have previously described analysis of both parallel and perpendicular hfc components from the ENDOR spectra of spin-labeled compounds to interpret the spectra in terms of principal dipolar hfc values and electron–nucleus distances.[7,8,14]

Molecular Modeling. Atomic coordinates of I were derived from X-ray defined molecular fragments by least-squares superposing the C(6), O(2), and N atoms of 2,2,5,5-tetramethyl-1-oxypyrroline-3-carboxamide[15] onto the C, O, and N atoms of the C-terminal peptide linkage of ethyl *N*-(bromoacetyl)-L-phenyl-

(10) Rozantsev, E. G. *Free Nitroxyl Radicals*; Plenum Press: New York, 1970; Chapter 9.

(11) Andersson, B. A.; Fölsch, G. *Chem. Scr.* **1972**, *2*, 21.

(12) Koch, T. R.; Kuo, L. C.; Douglas, E. G.; Jaffer, S.; Makinen, M. W. *J. Biol. Chem.* **1979**, *254*, 12310.

(13) (a) Yim, M. B.; Makinen, M. W. *J. Magn. Reson.* **1986**, *70*, 89. (b) Mustafi, D.; Makinen, M. W. *Inorg. Chem.* **1988**, *27*, 3360.

(14) Mustafi, D.; Wells, G. B.; Joela, H.; Makinen, M. W. *Free Radical Res. Commun.* **1990**, *10*, 95.

(15) Turley, W.; Boer, F. P. *Acta Crystallogr., Sect. B* **1972**, *28*, 1641.

TABLE I: Summary of Hfc Components (MHz) and Estimated Electron–Nucleus Distances (Å) of Methyl *N*-(2,2,5,5-Tetramethyl-1-oxypyrrolinyl-3-carbonyl)-L-phenylalanate in Frozen ($^2H_4$)Methanol

nucleus	$A_\parallel$	$A_\perp$	A_{iso}	$A_\parallel^D$	$A_\perp^D$	r^a
H^N	1.177	0.594	−0.004	1.181	−0.591	5.12 ± 0.03
H^α	0.534	0.262	0.003	0.531	−0.266	6.68 ± 0.04
$H^{\beta 1}$	0.380	0.181	0.006	0.374	−0.187	7.51 ± 0.15
$H^{\beta 2}$	0.242	0.138	−0.011	0.253	−0.127	8.56 ± 0.23
H^E	0.210	0.116	−0.007	0.217	−0.109	9.00 ± 0.30
$F^{\delta 1}$	0.240	0.133	−0.009	0.249	−0.125	8.43 ± 0.24
$F^{\delta 1'}$	0.520	0.398	−0.092	0.612	−0.306	6.25 ± 0.14[b]
F^ζ	0.202	0.100	0.001	0.201	−0.101	9.05 ± 0.29

[a] Uncertainty in frequency of ~0.010 MHz is included in the calculation of electron–nucleus distances. [b] Refers to the second conformation of the side chain observed as a species of low population on the basis of the peak-to-peak amplitudes in Figure 3.

TABLE II: Summary of Hfc Components (MHz) and Estimated Electron–Nucleus Distances (Å) of Methyl *N*-(2,2,5,5-Tetramethyl-1-oxypyrrolinyl-3-carbonyl)-L-phenylalanate in Frozen (^2H)Chloroform/($^2H_8$)Toluene

nucleus	$A_\parallel$	$A_\perp$	A_{iso}	$A_\parallel^D$	$A_\perp^D$	r^a
H^N	1.169	0.593	−0.006	1.175	−0.588	5.13 ± 0.02
H^α	0.524	0.260	0.001	0.523	−0.262	6.72 ± 0.12
$H^{\beta 1}$	0.449	0.258	−0.010	0.471	−0.236	6.95 ± 0.28
$H^{\beta 2}$	0.290	0.144	0.001	0.289	−0.145	8.18 ± 0.30
H^E	0.153	0.094	−0.012	0.165	−0.083	9.87 ± 0.36
$F^{\delta 1}$	0.189	0.107	−0.008	0.197	−0.099	9.11 ± 0.43
$F^{\delta 1'}$	0.486	0.336	−0.062	0.548	−0.274	6.48 ± 0.34[b]
F^ζ	0.164	0.096	−0.009	0.173	−0.087	9.51 ± 0.48

[a] Uncertainty in frequency of ~0.010 MHz is included in the calculation of electron–nucleus distances. [b] Refers to the second conformation of the side chain observed as a species of low population on the basis of the peak-to-peak amplitudes in Figure 3.

alanyl-L-phenylalanate.[16] This yielded a root-mean-square deviation of 0.022 Å for the superposed atoms. The C(3) atom of the spin label moiety was not used in the least-squares superposing because the C(3)–C(6) bond distance of 1.491 Å[15] differs significantly from the corresponding C^α–C bond distance of 1.630 Å in the reference phenylalanyl peptide.[16] Hydrogen coordinates were calculated for idealized geometries by using a C–H bond length of 1.09 Å and an N–H bond length of 1.00 Å. Fluorine substituents on the phenyl group were positioned with a C–F bond length of 1.30 Å.[17] The O–H bond length of the terminal carboxylate group in I′ was 0.98 Å.

Molecular modeling and torsional search calculations were carried out with use of the program package SYBYL,[18] running on an Evans & Sutherland PS390 graphics terminal. The basic elements and philosophy underlying the use of the program package have been described by Naruto et al.,[19a] and parameters for van der Waals contact radii were those of Iijima et al.[19b] With this program package, a systematic conformational analysis was carried out with SEARCH, which checks for van der Waals contacts among nonbonded atoms by scanning all possible torsional angles around rotatable bonds and identifies within van der Waals allowed conformational space those conformations that are compatible with specified ENDOR distances together with their respective uncertainties as added constraints.

Results and Discussion

ENDOR of Spin-Labeled Methyl L-Phenylalanate. The EPR absorption spectrum of a nitroxyl spin-label is a composite of three sets of spectral components of the nitroxyl group, differing by their projection of the ^{14}N nuclear moment onto the laboratory magnetic field $\mathbf{H}_0$ and designated by the values of $m_I = +1, 0, -1$. The low-field EPR spectral feature arises from molecules with $m_I = +1$, and the central feature in the EPR spectrum arises predominantly from molecules with $m_I = 0$. Microwave power saturation of the low-field feature (setting A) consequently selects molecules for ENDOR such that $\mathbf{H}_0$ is oriented perpendicular to the molecular plane of the spin-label, and saturation of the central feature (setting B) selects molecules of all orientations. For a nearby nucleus located in or near the molecular plane of the nitroxyl spin-label, setting A of $\mathbf{H}_0$ yields the perpendicular hf coupling, and setting B yields both the parallel and perpendicular hf couplings of a nucleus. On this basis, we have shown how selective saturation of these two EPR absorption features of spin-labels leads to a complete assignment of the ENDOR absorptions of nearby protons.[7,8,14] For purposes of brevity, we present ENDOR spectra collected under setting B of the static laboratory magnetic field since the perpendicular hf components identified under setting A are also included in the B setting spectra. However, assignment of all ENDOR absorptions presented in this study was made on the basis of analysis of spectra collected for both A and B settings.

In Figure 2 are shown proton ENDOR spectra of specifically deuterated analogues of spin-labeled methyl L-phenylalanate in ($^2H_4$)methanol. Each type of proton exhibits only two pairs of resonance features, indicating that the hf interaction is axially symmetric, and direct assignment of the origin of each ENDOR feature is readily made on the basis of selective deuteration. The spectrum of III consists of overlapping contributions of H^α and both $H^{\beta 1}$ and $H^{\beta 2}$ resonances. These are resolved in part through the spectrum of IV, which arises only from H^α, and on this basis the resonances of $H^{\beta 1}$ and $H^{\beta 2}$ are assigned in the spectrum of III. In ($^2H_4$)methanol exchange of the amide proton occurred rapidly in contrast to esters of other spin-labeled amino acids that we have investigated.[8] However, by rapid mixing of V in ($^2H_4$)methanol followed by immediate freezing, weak ENDOR features could be detected attributable to H^N. While these resonances for H^N could be assigned on this basis for I–VII in ($^2H_4$)methanol, the ENDOR resonances of the amide proton were readily determined for compounds I–VII in (^2H)chloroform:($^2H_8$)toluene (vide infra).

Previously we have observed that there is a pronounced change of side-chain conformation in spin-labeled methyl L-tryptophanate upon a change in solvent from methanol to chloroform:toluene.[8b] Therefore, we have compared the ENDOR spectra of spin-labeled methyl L-phenylalanate in these two solvents. The resonance features of the β protons for compounds I–VII in the polar and apolar solvent systems differ slightly, indicating a corresponding conformational alteration. We show later that this results in

(16) Wei, C. H.; Doherty, D. G.; Einstein, J. R. *Acta Crystallogr., Sect. B* **1972**, *28*, 907.

(17) Kennard, O. In *International Tables for X-ray Crystallography*; MacGillarry, C. H., Rieck, G. D., Eds.; Kynoch Press: Birmingham, U.K., 1968; Vol. 3, Section 4.2, pp 275–276.

(18) Marshall, G. R., personal communication. Detailed information on the use of this program package can be obtained from Tripos Associates, Inc., 1600 S. Hanley Road, St. Louis, MO 63144.

(19) (a) Naruto, S.; Motoc, J.; Marshall, G. R.; Daniels, S. B.; Sofia, M. J.; Katzenellenbogen, J. A. *J. Am. Chem. Soc.* **1985**, *107*, 5262. (b) Iijima, H.; Dunbar, J. B., Jr.; Marshall, G. R. *Proteins: Struct., Funct., Genet.* **1987**, *2*, 330.

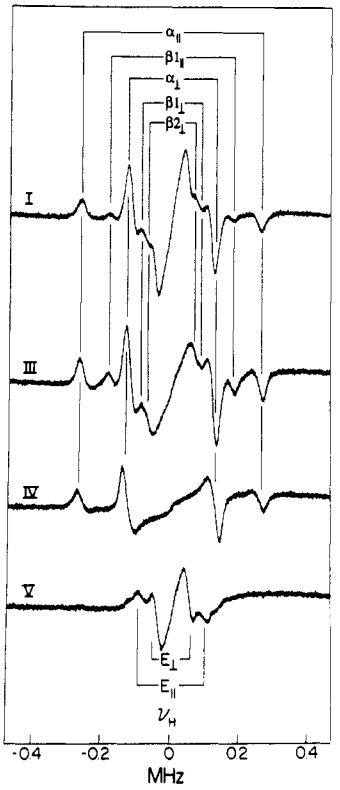

Figure 2. Proton ENDOR spectra of I and III–V in ($^2H_4$)methanol with H_0 at setting B of the EPR spectrum. For each class of protons, two line pairs are seen symmetrically spaced about the proton Larmor frequency at 14.33 MHz and are assigned to parallel and perpendicular hfc components. The abscissa indicates the ENDOR shift (measured ENDOR frequency minus free nuclear Larmor frequency). The ENDOR splittings are identified by stick diagrams for the H^α, H^β, and the H^E protons. In the spectrum of V, weak resonance features are observed adjacent to the $E_\perp$ features. These features coincide with those observed for the perpendicular hfc component of H^α, as is evident in the spectrum of IV. We ascribe these features to incomplete deuteration at the C^α position.

relatively small torsional rotational changes about the N–C^α and C^α–C^β bonds. In chloroform/toluene, proton ENDOR resonances were slightly better resolved than in methanol, due both to small shifts in the ENDOR splittings and somewhat narrower line widths. In Tables I and II we have summarized the ENDOR determined hfc constants for each class of nuclei and their corresponding electron–nucleus separations determined for I–VII in both solvent systems.

Figure 3 illustrates the ^{19}F ENDOR spectra of VI and VII in (^2H)chloroform:($^2H_8$)toluene for both magnetic field settings A and B. The spectra are centered at the ^{19}F Larmor frequency and are separated from most of the proton ENDOR features. The spectra for VII show well-resolved ENDOR features due to the fluorine substituent at the para position, and, within the limits of the signal-to-noise ratio, a single pair of resonance features is observed for the parallel and perpendicular splittings.

At the high-frequency side in Figure 3 there is a weak overlapping feature due to the vinylic proton of the oxypyrrolinyl ring, which tends to distort the ^{19}F ENDOR features. However, detailed comparison of the ^{19}F ENDOR spectra of VI consistently revealed four pairs of resonance features, one set being characterized by markedly greater peak-to-peak amplitudes. This observation suggests that the population of one conformation of the side chain with an ortho-fluorinated substituent is markedly greater than that of the other. We have previously observed similar sets of ^{19}F ENDOR absorptions for spin-labeled anilides with a fluorine substituent in the ortho position of the aromatic ring and have shown that they arise from two conformers obtained by rotation around the (aromatic)C–N bond.[7] On the other hand, a para substituent is not altered in position through a rotation around the C^β–C^γ bond, and only one pair of ENDOR features was observed for the parallel and perpendicular couplings of VII. In

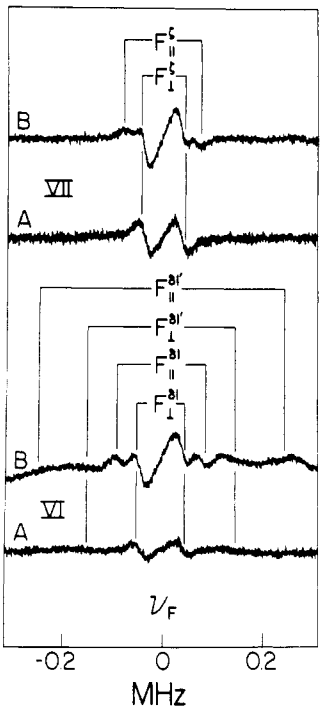

Figure 3. Fluorine ENDOR spectra of VI and VII in (^2H)chloroform/($^2H_8$)toluene for both magnetic field settings A and B. For the upper spectra for VII only two ENDOR line pairs can be identified. For the lower set of spectra for VI, one set of parallel and perpendicular line pairs is prominent while a second set of resonance features of low amplitude is evident. The diffuse features assigned to $F^{\delta 1'}$ were not altered substantially in relative intensity compared to those assigned to $F^{\delta 1}$ upon change of solvent from low (chloroform/toluene) to high (methanol) dielectric constant. Other conditions are as in Figure 2.

analogy to our earlier studies,[7,8b] we suggest that the added set of resonance features observed in the spectra of VI arise from a rotamer obtained by rotation of the side chain around the C^β–C^γ bond. We designate the conformational species of higher population as having an $F^{\delta 1}$ substituent, and the species of lower population is designated as having an $F^{\delta 1'}$ substituent. The values of the ^{19}F hfc components and their corresponding electron–nucleus separations are also summarized in Tables I and II.

The proton ENDOR spectra of VI and VII were identical within the limits of resolution with those observed for I, the resonance features of the aromatic protons being too diffuse for identification of the absent proton corresponding to the fluorine substituent. Since the proton splittings observed for VI and VII were identical with those of I, the addition of fluorine substituents has not altered the conformational properties of the spin-labeled phenylalanate ester. In addition, since the fluorophenylalanate esters employed as racemic mixtures yielded proton ENDOR spectra identical with that of I, the D enantiomer must have electron–nucleus separations identical with those of I.

ENDOR of Spin-Labeled L-Phenylalanine. In Figure 4 the proton ENDOR spectra of I′–V′ in ($^2H_4$)methanol are illustrated. The identification of resonances for $H^{\beta 1}$ and $H^{\beta 2}$ was made in a manner similar to that described for I–VII. For isotopically enriched analogues of I′ in methanol, however, it has been possible to identify the parallel hfc feature of $H^{\beta 2}$ by a careful comparison of the spectra of II′–IV′. This hfc component is the most difficult to identify, in general, because of its overlapping position with the perpendicular hfc feature of H^α. As noted earlier, the ENDOR resonance features of H^N were best detected for the spin-labeled methyl phenylalanate ester in the chloroform/toluene solvent system since amide proton exchange in ($^2H_4$)methanol was kinetically fast under the mixing conditions of sample preparation in these experiments. In Figure 4, the spectrum of V′ exhibits clearly resolved resonance features attributable only to H^N, indicating that amide proton exchange for this compound is significantly slower than for the methyl ester analogues. The spectrum of IV′ similarly shows the resonance features of H^N

TABLE III: Summary of Hfc Components (MHz) and Estimated Electron–Nucleus Distances (Å) in *N*-(2,2,5,5-Tetramethyl-1-oxypyrrolinyl-3-carbonyl)-L-phenylalanine in Frozen ($^2H_4$)Methanol

nucleus	$A_\parallel$	$A_\perp$	A_{iso}	$A_\parallel^D$	$A_\perp^D$	r^a
H^N	1.167	0.604	−0.014	1.180	−0.590	5.12 ± 0.03
H^α	0.523	0.259	0.002	0.521	−0.261	6.72 ± 0.05
$H^{\beta 1}$	0.377	0.179	0.006	0.371	−0.186	7.53 ● 0.10
$H^{\beta 2}$	0.251	0.138	−0.008	0.259	−0.130	8.48 ± 0.24
$F^{\delta 1}$	0.232	0.136	−0.013	0.245	0.123	8.47 ± 0.36
$F^{\delta 1'}$	0.509	0.328	−0.049	0.555	0.278	6.45 ± 0.11[b]
F^ζ	0.198	0.099	0.000	0.198	−0.099	9.10 ± 0.22

[a] Uncertainty in frequency of ~0.010 MHz is included in the calculation of electron–nucleus distances. [b] Refers to the second conformation of the side chain observed as a species of low population on the basis of the peak-to-peak amplitudes in Figure 3.

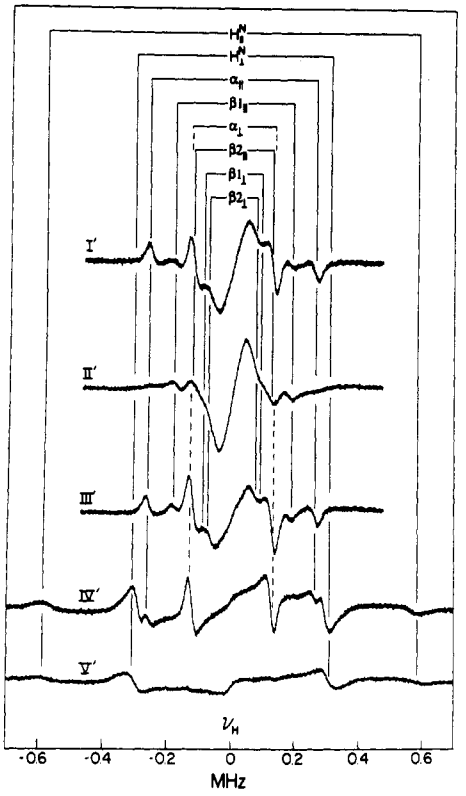

Figure 4. Proton ENDOR spectra of compounds I′–V′ in ($^2H_4$)methanol at setting B. The ENDOR splittings for H^N are shown only in the spectra of IV′ and V′. These two samples were prepared by rapid mixing of compounds in ($^2H_4$)methanol followed by immediate freezing. Conditions are, in general, as indicated in Figure 2.

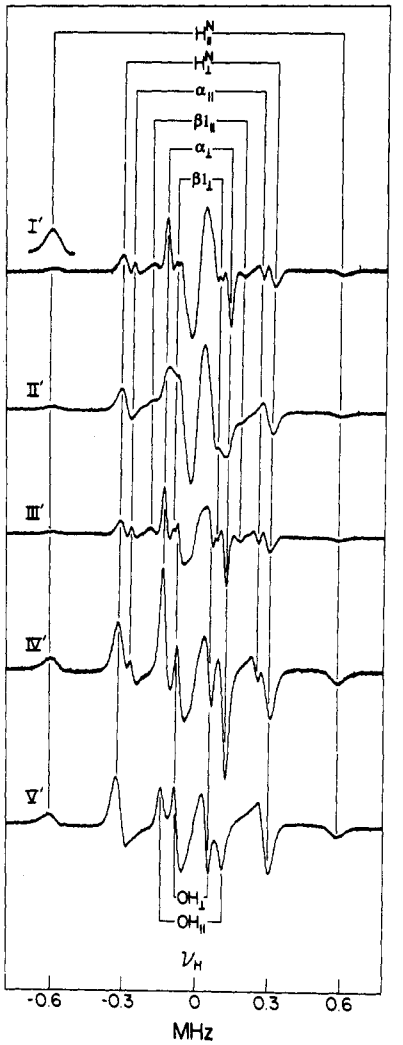

Figure 5. Proton ENDOR spectra of compounds I′–V′ in ($^2H_6$)-DMSO:(^2H)chloroform:($^2H_8$)toluene with H_0 at setting B. For spectra I′–III′ lower depth modulation of the rf field was used than for IV′ and V′ to separate overlapping contributions. The relative depth modulation employed for spectra I′–III′ and IV′ and V′ can be gauged from the amplitudes of the H^N resonance features. The ENDOR line pairs are identified for each type of proton by the stick diagrams.

together with the ENDOR absorptions of H^α. In this case the perpendicular absorption of H^N is better separated from the parallel absorption of H^α than it is in the case of spin-labeled methyl phenylalanate.

In Figure 5 we have illustrated the proton ENDOR spectra of selectively deuterated analogues of spin-labeled L-phenylalanine in the aprotic ternary solvent ($^2H_6$)DMSO:(^2H)chloroform:($^2H_8$)toluene. In this ternary solvent mixture, the resonance features of I′–VII′ were markedly sharper and of greater peak-to-peak amplitude and higher signal-to-noise ratio than with use of the binary chloroform/toluene solvent. Since the addition of DMSO to the binary solvent made no noticeable change in the quality of the ENDOR spectra of spin-labeled methyl phenylalanate, we conclude that compounds I′–VII′ are less soluble or perhaps not monodisperse in the apolar, binary chloroform/toluene solvent. The use of compound V′ in the aprotic ternary solvent provided an unusual opportunity to detect the resonances of the two polar protons H^N and H^{OH} that normally are exchanged in methanol. Assignment of the hfc components of H^{OH} thus allows us to make a direct comparison of the conformation of the carboxylic acid group with that of the methyl carboxylate group of I.

In Figure 6 are illustrated the ^{19}F ENDOR spectra of VI′ and VII′ in the same aprotic ternary solvent mixture. The resonance features are well resolved for the predominant conformational species. As for VI in Figure 3, weak, unresolved absorption was also detected for VI′ belonging to a conformational species of low population, and the relative intensities of the two sets of resonance features were not markedly altered upon change of the solvent to ($^2H_4$)methanol. A summary of the ENDOR determined hfc constants of both types of nuclei in I′–VII′ with corresponding electron–nucleus separations is given in Tables III and IV.

Molecular Modeling of Spin-Labeled Methyl L-Phenylalanate. To determine the conformations of spin-labeled methyl L-phenylalanate and of L-phenylalanine, we have carried out a conformational search of the limits of the torsion angles for rotation around the C(3)–C(6) and C(6)–N bonds within the

TABLE IV: Summary of Hfc Components (MHz) and Estimated Electron–Nucleus Distances (Å) of *N*-(2,2,5,5,-Tetramethyl-1-oxypyrrolinyl-3-carbonyl)-L-phenylalanine in Frozen ($^2H_6$)Dimethyl Sulfoxide/(^2H)Chloroform/($^2H_8$)Toluene

nucleus	$A_\parallel$	$A_\perp$	A_{iso}	$A_\parallel^D$	$A_\perp^D$	r[a]
H^N	1.190	0.619	−0.016	1.206	−0.603	5.08 ± 0.02
H^α	0.528	0.251	0.009	0.523	−0.262	6.72 ± 0.02
$H^{\beta 1}$	0.370	0.177	0.005	0.367	−0.183	7.57 ● 0.05
$H^{\beta 2}$	0.282	0.130	0.007	0.275	−0.137	8.32 ± 0.16
H^{OH}	0.254	0.138	−0.007	0.261	−0.131	8.46 ± 0.11
$F^{\delta 1}$	0.215	0.113	−0.004	0.219	−0.109	8.79 ± 0.12
F^{ζ}	0.176	0.099	−0.007	0.183	−0.092	9.34 ± 0.30

[a] Uncertainty in frequency of ~0.010 MHz is included in the calculation of electron–nucleus distances.

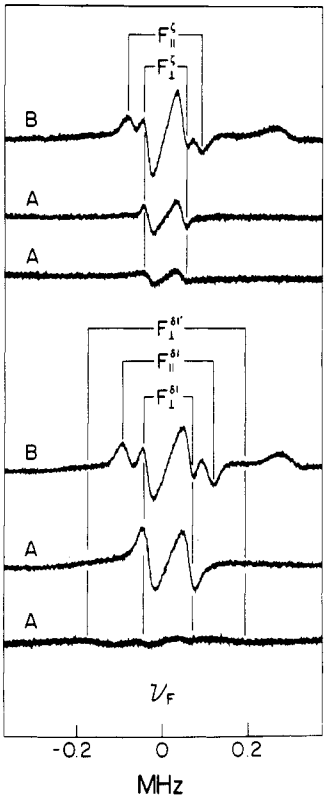

Figure 6. Fluorine ENDOR spectra of VI′ and VII′. The upper set of spectra belong to compound VII′, and the lower set are from VI′. For each set of three spectra, the lowermost spectrum is for the compound in (^2H)chloroform/($^2H_8$)toluene, and the upper two spectra are for the spin-labeled fluorophenylalanine derivative in ($^2H_6$)DMSO/(^2H)chloroform/($^2H_8$)toluene to illustrate the markedly reduced intensities observed for I′–VII′ in the binary solvent. The resonance features associated with the conformation of low population are less prominent than their counterparts of VI in Figure 3.

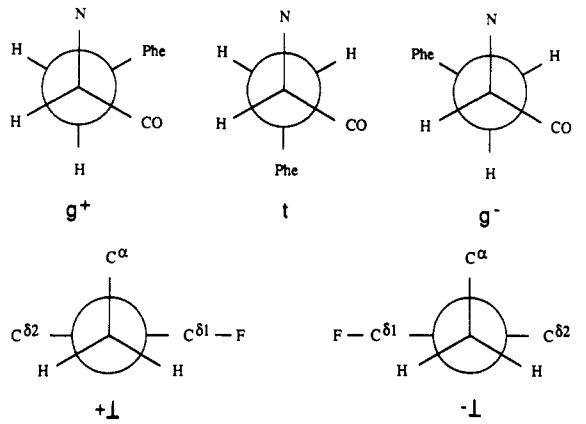

Figure 7. Newman diagrams of the gauche$^+$ (g^+), trans (t), and gauche$^-$ (g^-) conformations of L-phenylalanine. The dihedral angle relationships for χ_1 are shown in the upper part, while the relationships for χ_2 indicating perpendicular (+⊥) and antiperpendicular (−⊥) conformations are shown in the lower part. For the ortho-fluorine substituent we have elected to designate the carbon atom to which it is covalently bonded as $C^{\delta 1}$. Comparison of the side-chain orientations of I and I′ to those of methyl L-tryptophanate,[8b] as in Table V, then results in opposite signs for values of χ_2 for perpendicular and antiperpendicular orientations. This circumstance results, thus, only from nomenclature and does not indicate a difference in preferred conformation.

spin-label acyl moiety and around the N–C^α, C^α–C^β, C^β–C^γ, C^α–C, and C–O″ bonds within the phenylalanyl moiety, constrained to the electron–nucleus distances summarized in Tables I–IV. The general methodology employed in these calculations has been described in our earlier publications,[7,8] and the effective position of the unpaired spin density of the nitroxyl group as a point dipole was assigned as earlier for the spin-label carboxamide derivative.[8,20]

For purposes of molecular modeling, several conventions for the choice of van der Waals radii have been applied.[21-23] The choices in general depend on whether to explicitly consider the contribution of covalently bonded hydrogens or to account for their contributions by assigning an appropriate radius to the heavy-atom nucleus, resulting in a spherically symmetric, expanded atom. To develop criteria for application of ENDOR distance constraints, we have compared the results of torsion angle calculations to simulate the X-ray-defined structure of 2,2,5,5-tetramethyl-1-oxypyrroline-3-carboxamide,[15] applying the electron–proton distance constraints to the vinylic proton and to the two carboxamide protons determined in earlier studies.[14,20] For this comparison we employed the van der Waals radii of Iijima et al.,[18,19b,24] in which hydrogen atoms are explicitly considered, and the van der Waals radii of Bondi,[22] in which the heavy-atom radii are spherically expanded to account for covalently bonded hydrogens. The use of Bondi's van der Waals radii resulted in a two-fold degeneracy of the molecular conformation so that the tilt of the plane of the carboxamide group with respect to the plane of the oxypyrrolinyl ring as defined by the [C(4)–C(3)–C(6)–N] torsion angle was −45° or +20°. The use of the parameters by Iijima et al.[19b] gave only one conformation with a value of −39° for the torsion angle. The value of this angle calculated from atomic coordinates is −30°.[15] On this basis, we have employed the van der Waals parameters of Iijima et al.[19b] to assign the conformations of I and I′, according to experimentally determined ENDOR electron-nucleus distance constraints. For the $F^{\delta 1}$-substituted phenylalanine, we have restricted the analysis primarily to the conformational species of highest population with an electron–fluorine separation of ~8.5 Å (cf. Tables I–IV). Important differences for the species of lower population are presented where relevant.

(20) Mustafi, D.; Joela, H.; Makinen, M. W. *J. Magn. Reson.* **1991**, *91*, 497.
(21) Ramachandran, G. N.; Sasisekharan, V. *Adv. Prot. Chem.* **1968**, *23*, 284.
(22) (a) Bondi, A. *Physical Properties of Molecular Crystals, Liquids, and Glasses*; Wiley: New York, 1988. (b) Bondi, A. *J. Phys. Chem.* **1964**, *68*, 441.
(23) Richards, F. M. *Annu. Rev. Biophys. Bioeng.* **1977**, *6*, 151.
(24) The van der Waals radius of an element in the listing of Iijima et al.[19b] is defined as $r_w = b + 0.76$, where b is the covalent radius of the atom. This definition is that originally put forth by Pauling.[25]
(25) Pauling, L. *The Nature of the Chemical Bond*, 3rd ed.; Cornell University Press: Ithaca, NY, 1960; Chapter 7.

TABLE V: Comparison of Dihedral Angles of the X-ray-Defined Reference Molecular Model and of the ENDOR-Constrained Conformations of Spin-Labeled L-Phenylalanine, Spin-Labeled Methyl L-Phenylalanate, and Spin-Labeled Methyl L-Tryptophanate

dihedral angle	ref molecular model[a]	conformations found[b] L-phenylalanine MeOH	L-phenylalanine D/C/T[c]	methyl L-phenylalanate MeOH	methyl L-phenylalanate D/C/T[c]	methyl L-tryptophanate[d] MeOH	methyl L-tryptophanate[d] C/T[c]
Without Hydrogen Atoms							
[C(4)-C(3)-C(6)-O(2)]	149	140 ± 5	134 ± 6	139 ± 5	139 ± 5	138 ± 2	130 ± 2
[C(4)-C(3)-C(6)-N]	-30	-38 ± 5	-45 ± 6	-40 ± 5	-40 ± 5	-42 ± 2	-50 ± 2
[C(3)-C(6)-N-C^{α}]	-177	-178 ± 3	-176 ± 3	-174 ± 3	-174 ± 3	-176 ± 2	-177 ± 3
[O(2)-C(6)-N-C^{α}]	4	4 ± 3	6 ± 3	7 ± 3	7 ± 3	4 ± 2	3 ± 3
[C(6)-N-C^{α}-C]	-122	-77 ± 8	-76 ± 8	-78 ± 8	-112 ± 5	-66 ± 6	-87 ± 7
[C(6)-N-C^{α}-C^{β}]	126	170 ± 8	172 ± 8	170 ± 8	135 ± 5	172 ± 6	151 ± 7
[N-C^{α}-C^{β}-C^{γ}]	-72	-72 ± 5	-72 ± 5	-75 ± 5	-100 ± 5	-63 ± 2	-95 ± 5
[C-C^{α}-C^{β}-C^{γ}]	176	175 ± 5	175 ± 5	172 ± 5	147 ± 5	174 ± 2	142 ± 5
[C^{α}-C^{β}-C^{γ}-$C^{\delta 1}$]	-92	-73 ± 5	-78 ± 5	-73 ± 5	-83 ± 5	105 ± 5	-105 ± 8
[C^{α}-C^{β}-C^{γ}-$C^{\delta 2}$]	96	115 ± 5	110 ± 5	115 ± 5	105 ± 5	-73 ± 5	77 ± 8
With Hydrogen Atoms							
[O(2)-C(6)-N-H^{N}]	-176	-177 ± 3	-175 ± 3	-173 ± 3	-173 ± 3	-176 ± 2	-177 ± 3
[C(3)-C(6)-N-H^{N}]	3	2 ± 3	4 ± 3	6 ± 3	6 ± 3	4 ± 2	-16 ± 3
[H^{N}-N-C^{α}-H^{α}]	180	-136 ± 8	-134 ± 8	-136 ± 8	-171 ± 5	-127 ± 6	-148 ± 7
[H^{N}-N-C^{α}-C^{β}]	-54	-10 ± 8	-9 ± 8	-10 ± 8	-45 ± 5	-8 ± 6	-29 ± 7
[N-C^{α}-C^{β}-$H^{\beta 1}$]	169	169 ± 5	169 ± 5	166 ± 5	166 ± 5	177 ± 2	145 ± 5
[C-C^{α}-C^{β}-$H^{\beta 1}$]	56	56 ± 5	56 ± 5	53 ± 5	28 ± 5	54 ± 2	23 ± 5
[H^{α}-C^{α}-C^{β}-$H^{\beta 1}$]	-66	-66 ± 5	-66 ± 5	-69 ± 5	-93 ± 5	-66 ± 2	-97 ± 5
[H^{α}-C^{α}-C^{β}-C^{γ}]	53	53 ± 5	53 ± 5	50 ± 5	25 ± 5	55 ± 2	24 ± 5
[$H^{\beta 1}$-C^{β}-C^{γ}-$C^{\delta 1}$]	27	46 ± 5	40 ± 5	45 ± 5	36 ± 5	-135 ± 5	15 ± 8
[$H^{\beta 1}$-C^{β}-C^{γ}-$C^{\delta 2}$]	-146	-127 ± 5	-132 ± 5	-127 ± 5	-137 ± 5	45 ± 5	-162 ± 8

[a] Atomic coordinates of the reference molecular model were derived from X-ray-defined fragments,[15,16] as described in the text. Values of dihedral angles are given in degrees. [b] Results are provided only for the predominant conformation found for compounds VI, VII, viz., VI', VII' in frozen solutions of methanol and DMSO/chloroform/toluene. [c] D/C/T refers to the DMSO/chloroform/toluene ternary solvent mixture; correspondingly C/T refers to the binary chloroform/toluene solvent. [d] Values of dihedral angles are taken from ref 8b.

To assign side-chain conformation, we have employed the electron–fluorine distance constraints for both the $F^{\delta 1}$ and the F^{ζ} substituents and for a hypothetical $F^{\delta 1}$,F^{ζ}-difluoro-substituted phenyl group for which the two electron–fluorine distance constraints are applied simultaneously. Because the $F^{\delta 1}$ substituent lifts the mirror symmetry of the benzyl group along the C^{β}–C^{γ} bond, side-chain conformers that differ by rotation around the C^{β}–C^{γ} bond must also be considered. On this basis the disposition of the $F^{\delta 1}$ substituent is described with respect to the [C^{α}–C^{β}–C^{γ}–$C^{\delta 1}$][26] torsion angle corresponding to perpendicular and antiperpendicular conformations in a manner similar to defining the χ_2 angle for the side chain of tryptophan.[8b] These relationships are schematically illustrated in Figure 7.

The results of the conformational search calculations are illustrated in part in Figure 8. In this diagram the conformational space accessible to the molecule under van der Waals and ENDOR distance constraints is illustrated for rotation around the C^{α}–C^{β} (χ_1) and the C^{β}–C^{γ} (χ_2) bonds for spin-labeled L-phenylalanine in the ternary DMSO/chloroform/toluene solvent. As is evident, successive application of the proton distance constraints yields a corresponding decrease in the ENDOR compatible conformational space. However, the most marked reduction in the ENDOR compatible conformational space is observed by simultaneous application of both electron–fluorine distance constraints together with the four electron–proton separations. In Figure 8 it is seen that regions corresponding to g^+, t, and g^- conformers are sterically allowed for both perpendicular and antiperpendicular conformations of an ortho-fluorinated side chain while application of the electron–proton distance constraints restricts the accessible conformational space to only the g^- manifold. The addition of the F^{ζ} distance constraint does not alter this result, as expected, whereas application of the $F^{\delta 1}$ distance constraint of ~8.5 Å limits the accessible space to the g^-, antiperpendicular conformation.

From such torsion angle calculations molecular models were constructed according to the mean values of the dihedral angles for spin-labeled methyl L-phenylalanate and spin-labeled L-phenylalanine in each solvent. The mean values of each dihedral angle and their corresponding line-width-based uncertainties are summarized in Table V. The results show that the conformations of the spin-label group and of the side chain of spin-labeled L-phenylalanine are essentially identical in both solvents, and these values are nearly identical with values of the corresponding dihedral angles of the methyl ester in methanol. As seen in Table V the results for L-phenylalanine and for its methyl ester are in good agreement with the X-ray-defined molecular model. These results show, furthermore, that the conformations of spin-labeled L-phenylalanine, methyl L-phenylalanate, and methyl L-tryptophanate[8b] in methanol are comparable to each other. The structural similarity of spin-labeled methyl L-phenylalanate and of methyl L-tryptophanate is illustrated in Figure 9. On the other hand, comparison of the dihedral angles of spin-labeled methyl

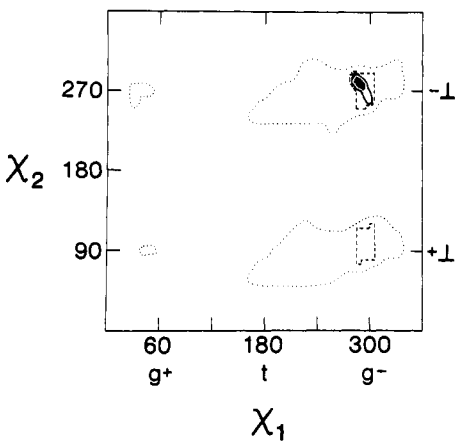

Figure 8. Angle maps of χ_1 and χ_2 for VI' and VII' as a function of ENDOR-determined distance constraints. The axes representing values of χ_1 and χ_2 are indicated in degrees and values are labeled on the axes for the classical conformers illustrated in Figure 7. The conformational space is indicated according to the following distance constraints: only van der Waals constraints (···); H^{N}, H^{α}, $H^{\beta 1,2}$ (– – –); H^{N}, H^{α}, $H^{\beta 1,2}$, $F^{\delta 1}$ (—); H^{N}, H^{α}, $H^{\beta 1,2}$, $F^{\delta 1}$, F^{ζ} (solid area). Each set of ENDOR distance constraints were applied together with van der Waals hard-sphere limits as discussed in the text.

(26) The conventions and nomenclature used are those described by the IUPAC-IUB Commission on Biochemical Nomenclature: *Biochemistry* **1970**, *9*, 3471.

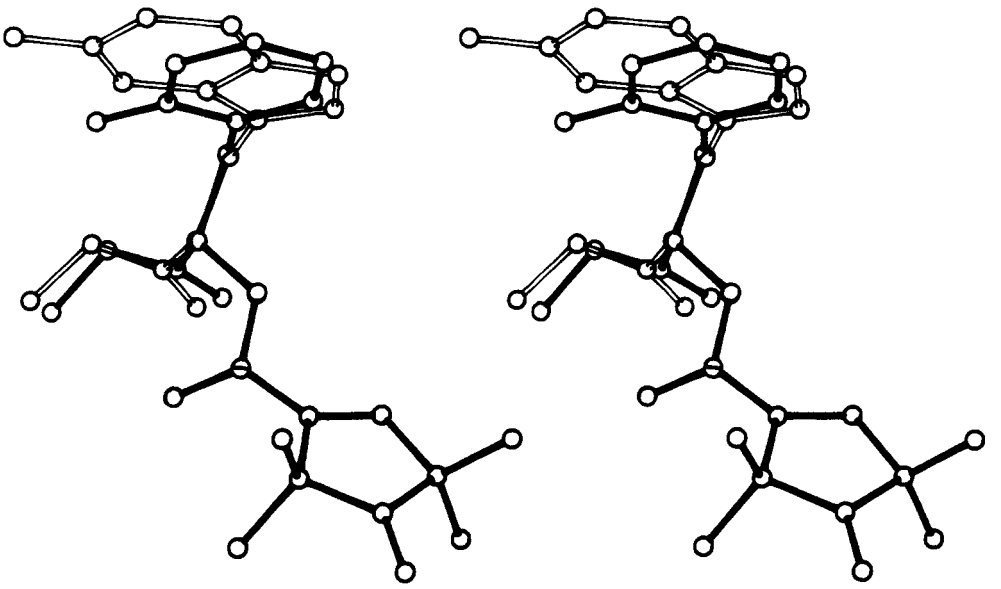

Figure 9. Stereodiagram comparing the structure of the $g^-,-\perp$ conformer of compound VI to the "extended" conformation of spin-labeled methyl L-β3-fluorotryptophanate.[8b] With respect to the dihedral angle χ_2, it is seen that the ortho-fluorine substituent of VI is in an $-\perp$ orientation, and the "extended" conformer of the tryptophan side chain is in a $+\perp$ orientation. The methyl carboxylate group is shown for both spin-labeled amino acid esters according to the θ, ψ dihedral angles of ~245°, 155°, similar to the ϕ, ψ values of a peptide group in a fully extended conformation. Compound VI is represented by solid bonds while the tryptophan moiety is illustrated with open bonds. The two ENDOR-determined structures are superposed only according to the six atoms of the oxypyrrolinyl ring.

L-phenylalanate in the DMSO/chloroform/toluene ternary solvent shows that they differ in part from the corresponding values of the molecule in methanol but are more nearly comparable to those exhibited by spin-labeled methyl L-tryptophanate[8b] in chloroform/toluene.

It is of importance to note that the ENDOR-determined structure of spin-labeled methyl L-phenylalanate is in good agreement not only with the reference phenylalanyl peptide model,[16] as seen in Table V, but also with that of *N*-acetyltaurylmethyl L-phenylalanate crystallized from ethyl acetate.[27] Although our estimates of the dihedral angle χ_2 of the side chain must be necessarily assigned through use of the L-δ-fluorophenylalanine derivative, the χ_2 angles measured with respect to the $C^{\delta 1}$ and $C^{\delta 2}$ atoms in Table V for I in the apolar solvent are in good agreement with those of 84.5° and −95.0° for *N*-acetyltaurylmethyl L-phenylalanate.[27] Also, in the tauryl derivative the side chain is in a staggered g^- conformation with $\chi_1 = -67.5°$, and the values of the dihedral angles corresponding to ϕ, ψ in a peptide are −102°, 166°, in excellent agreement with those of −112°, 155° in the ENDOR-determined structure of I.

In Figure 10 we have illustrated the angle map for rotation around the C^α–C and C–O″ bonds to assign the conformation of the –COOH group in compounds I′–VII′ and of the $-COOCH_3$ group in compounds I–VII. Application of the distance constraint of 8.46 ± 0.11 Å to H^{OH} markedly reduces the accessible conformational space. The narrow band of ENDOR-compatible conformational space covering a range of 0–360° in θ arises from the circumstance that, for the corresponding range of values for ψ, rotation around the C–O″ bond keeps the carboxylic acid proton essentially equidistant from the nitroxyl group. Three conformations of the –COOH group are allowed by the exact values of the ENDOR distance constraints, including that of 8.46 Å to H^{OH}. These structures are similar to the three families of conformations observed for the $-COOCH_3$ group in compounds I–VII, which, in turn, as shown in Figure 10, are identical with those observed for spin-labeled methyl L-alanate[8a] and spin-labeled methyl L-tryptophanate.[8b] Region 1 associated with a value of ψ of ~280° (−80°) corresponds to ψ in a right-handed α-helical polypeptide,[8a] while region 2 near ψ of 170° is close to that observed in fully extended conformations. This latter conformer

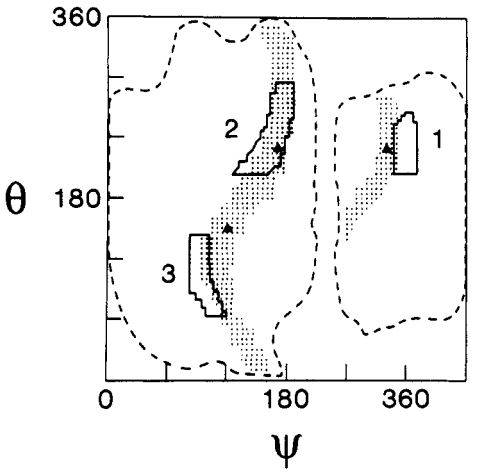

Figure 10. Comparison of torsion angle maps of the carboxylic acid and methyl carboxylate groups of I′ and I, respectively. The axes labeled as θ and ψ represent 0–360° rotation around the C–O″ and C^α–C bonds, respectively. The large conformational space indicated by broken lines is compatible with nonbonded van der Waals constraints. Three regions of conformational space, indicated by numbers 1–3, compatible with the ENDOR distance constraint to the averaged ester methyl protons (H^E) is represented by a closed solid line for I. The conformational space represented by dots is for I′ with the distance constraint of 8.46 ± 0.11 Å to H^{OH}. Three conformations indicated by filled triangles are found for the –COOH group of I′ by using exact values of ENDOR distance constraints, as listed in Table IV.

is of lowest potential energy for the $-COOCH_3$ group in methanol.[28]

It is of interest to note that the major conformer of the ortho-fluorinated side chain is found as $g^-,-\perp$ although the $g^-,+\perp$ conformer is sterically permitted, and evidence for low population of this species is seen in Figures 3 and 6. The preferred conformation of the ortho-fluoro substituent with an electron–$F^{\delta 1}$ separation of ~8.5 Å can be explained on the basis of dipolar interactions in the molecule in a manner similar to that employed in our earlier study of methyl L-tryptophanate.[8b] To model the dipolar contribution of the *o*-fluorobenzyl side chain, we have

(27) Calcagni, A.; Gavuzzo, E.; Lucente, G.; Mazza, F.; Pochetti, G.; Rossi, D. *Int. J. Peptide Protein Res.* **1989**, *34*, 319.

(28) Romanowski, H.; Makinen, M. W., manuscript in preparation.

TABLE VI: Geometrical Relationships and Estimated Dipolar Interaction Energies of the Dipoles of the Peptide Bond, $F^{\delta 1}$-Benzyl Group, and the Methyl Carboxylate Group in Spin-Labeled Methyl L-Phenylalanate[a]

conformer[b,c]	dipoles	dipole–dipole separation, Å	angle,[d] deg	dipolar energy, kcal/mol	total energy,[e,f] kcal/mol	fraction[g]
$g^-,-\perp$	peptide and $F^{\delta 1}$-benzyl group	4.65	88.0	0.058		
		(4.65)	(88.0)	(0.058)		
					−0.293	0.89
	carboxylate and $F^{\delta 1}$-benzyl group	5.08	97.8	−0.351	(0.134)	(0.37)
		(5.09)	(24.7)	(0.077)		
$g^-,+\perp$	peptide and $F^{\delta 1}$-benzyl group	4.63	113.5	0.238		
		(4.63)	(113.5)	(0.238)		
					0.413	0.11
	carboxylate and $F^{\delta 1}$-benzyl group	4.89	58.2	0.175	(−0.041)	(0.63)
		(4.89)	(151.0)	(−0.279)		

[a] Calculated for electric dipoles, as defined for *o*-fluorotoluene,[29,30] the carboxylate group,[31a] and the peptide bond.[31] [b] The $g^-,-\perp$ conformer has χ_1 and χ_2 values of −100° and −83°, respectively, whereas for the $g^-,+\perp$ conformer the dihedral angles have values of −110° and 97°, respectively. In the $g^-,-\perp$ and in the $g^-,+\perp$ conformer the electron-to-$F^{\delta 1}$ distances are 9.11 and 6.48 Å, respectively, as listed in Table II. [c] In this calculation both conformations belonging in Figure 10 to region 1 (α-helical-like) and region 2 (fully extended) of the carboxylate group are employed, and the interaction energies with the fluorobenzyl group are calculated for both ester conformers. The dihedral angles, θ and ψ, that describe the orientation of the carboxylate group (cf. Figure 10), have values of −132°, −57° and −115°, 155°, for regions 1 and 2, respectively. These conformations of the carboxylate group are compatible with the ENDOR determined electron–proton distance to the methyl protons of the carboxylate group. In earlier studies we have shown that among the three ENDOR allowed conformations of the carboxylate group these two in methanol are of lowest energy.[8a,28] The values in the parentheses are for the ester conformation that corresponds to the dihedral angles θ, ψ of −132°, −57° in region 1 and is thus similar to that of peptide group in an α-helix. [d] Angle between indicated dipoles. [e] The interaction energy between the dipoles[31] of the peptide bond and the carboxylate group is −3.427 and +3.416 kcal/mol for the fully extended and α-helical-like conformations of the $-COOCH_3$ group, respectively. [f] Total dipolar interaction energies are estimated as the sum of each dipolar interaction energy. [g] The fraction of relative populations are calculated at −100 °C to approximate the freezing temperature of the solvents employed in this investigation.

applied the experimentally determined dipoles of toluene and fluorobenzene.[29,30] This produces a resultant dipole of 1.45 D directed 107° away from the C^γ–C^ζ axis in the benzene ring and away from the ortho-fluoro substituent. In preliminary studies we have found that the conformations of methyl esters of spin-labeled amino acids in regions 1 and 2 of Figure 10 are lower in potential energy by approximately 4 kcal/mol than that of region 3.[8a,28] We have, therefore, evaluated fluorobenzyl dipolar interactions in spin-labeled methyl phenylalanate with carboxylate structures corresponding to regions 1 and 2 of Figure 10. A summary of the calculated results is given by Table VI.

In Table VI it is seen that the interaction of the ester group is the determinant of the orientation of the fluorobenzyl side chain. With a fully extended $-COOCH_3$ group the $g^-,-\perp$ orientation is energetically favored over the $g^-,+\perp$ orientation by a factor of approximately 8:1 in population. This result can be qualitatively understood through Figure 11. The peptide and ester dipoles are placed into near antiparallel orientations for a fully extended carboxylate group, effectively compensating each other. In the $g^-,-\perp$ conformer, the fluorobenzyl dipole is more nearly perpendicular to the ester dipole, but in the $g^-,+\perp$ conformer it is more nearly parallel to the ester dipole. The near-parallel orientation raises the potential energy of the molecule, resulting in its lower population.

On the other hand, with an α-helical-like conformation of the $-COOCH_3$ group, the $g^-,+\perp$ orientation is calculated as predominant with a fractional population of 0.63. This species would be characterized by an approximate 6.5-Å electron–$F^{\delta 1'}$ separation. In Figures 3 and 6 for both solvents the predominant spectral species of VI and VI′, respectively, can be accounted for only by the $g^-,-\perp$ fluorobenzyl side chain corresponding to an approximate 8.5–9.0-Å electron–$F^{\delta 1}$ separation. Thus, the experimental observations directly rule out the $g^-,+\perp$ conformer as the major species and consequently indicate that the predominant conformation of the carboxylate group corresponds to that of a fully extended structure. As evident in Figure 10, the electron–H^E distance constraint identifies three ENDOR compatible families of conformers of the $-COOCH_3$ group. The results in Table VI indicate that only region 2 is energetically favored, and we

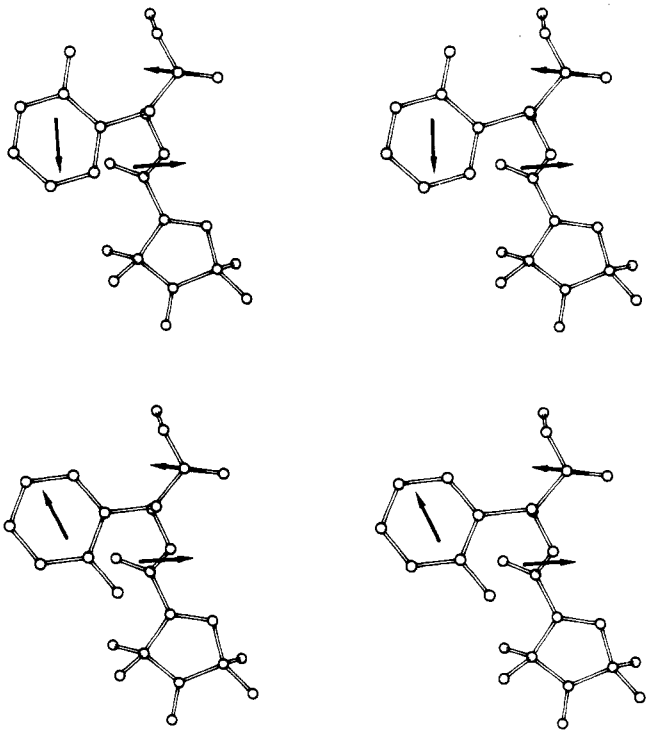

Figure 11. Stereodiagram of the $g^-,-\perp$ (upper) and $g^-,+\perp$ (lower) conformers of I calculated according to ENDOR distance constraints and drawn to illustrate the electric dipoles of the *o*-fluorobenzyl side chain and of the ester and peptide groups. The dipoles are represented as arrows with a length of 1.2 Å each centered on their respective midpoints.

therefore assign the structure of I and I′ to the fully extended carboxylic acid function.

Our assignment of the $g^-,-\perp$ conformer of the *o*-fluorobenzyl side chain may be of relevance to the use of fluorophenylalanine incorporated biosynthetically in proteins for NMR studies.[32] While both perpendicular and antiperpendicular conformers of an *o*-fluorobenzyl side chain are sterically allowed, our results indicate that the preferred conformation of the *o*-fluorobenzyl side chain is antiperpendicular for an extended $-COOCH_3$ group. This

(29) Catalán, J.; Macias, A. *J. Mol. Struct.* **1977**, *38*, 209.
(30) (a) Moore, E. M.; Hobbs, M. E. *J. Am. Chem. Soc.* **1949**, *71*, 411. (b) McClellan, A. L. *Tables of Experimental Dipole Moments*; W. H. Freeman: San Francisco, CA, 1963; pp 245–251.
(31) (a) Wada, A. *Adv. Biophys.* **1976**, *9*, 1. (b) Hol, W. G. J.; van Duijnen, P. T.; Berendsen, H. J. C. *Nature* **1978**, *273*, 443.
(32) (a) Sykes, B. D.; Weiner, J. H. In *Magnetic Resonance in Biology*; Cohen, J. S., Ed.; Wiley: New York, 1980; Vol. 1, pp 171–196. (b) Gerig, J. T.; Klinkenborg, J. C.; Nieman, R. A. *Biochemistry* **1983**, *22*, 2076.

conformation of the carboxylate group corresponds to that of a peptide in a fully extended β-sheet structure. However, in Table IV, the calculated electrostatic dipole–dipole interactions suggest that the preferred conformation of an *o*-fluorobenzyl side chain is perpendicular when the carboxylate (or, correspondingly, peptide) group is in an α-helical conformation. Helix–coil transitions in a protein in which L-δ-fluorophenylalanine is incorporated would thus lead to a change in side chain orientation. While for normal proteins this leads to no structural alteration in side-chain conformation, the reorientation of the bulkier ortho-fluoro substituent may lead to destabilizing effects in the protein. It is also of considerable interest to note that incorporation of ortho, meta, or para isomers of L-fluorophenylalanine into gramicidin can result in more than a 2.5-fold variation in the Na^+ ion conductance of gramicidin channels.[33] The influence of the fluorophenyl isomer on Na^+ ion conductance is explained on the basis of alteration of the energy profile of permeating ions by electrostatic interactions of the side-chain dipoles. It is probable that the isomer dependent dipole interaction of fluorophenylalanine with permeating ions in gramicidin channels is of an origin identical with the orientationally dependent dipole interactions calculated for spin-labeled methyl L-phenylalanate in Table VI.

Registry No. I, 135823-85-7; I′, 70290-92-5; II, 135823-86-8; III, 135823-87-9; III′, 135823-91-5; IV, 135852-96-9; V, 135823-88-0; VI, 135823-89-1; VII, 135823-90-4; H-Phe-OMe·HCl, 7524-50-7; 2,2,5,5-tetramethyl-1-oxypyrrolinylcarboxylic acid chloride, 13810-21-4; L-($\delta1,\delta2,\epsilon1,\epsilon2,\delta$-$^2H_5$)-phenylalanine, 56253-90-8.

(33) Koeppe, II, R. E.; Mazet, J. L.; Andersen, O. S. *Biochemistry* **1990**, *29*, 512.

Intramolecular Photoassociation and Photoinduced Charge Transfer in Bridged Diaryl Compounds. 1. Photoassociation in the Lowest Triplet State of 2,2′-Dinaphthylmethane and 2,2′-Dinaphthyl Ether

Steven H. Modiano, Jozef Dresner,† and Edward C. Lim*,‡

Department of Chemistry, The University of Akron, Akron, Ohio 44325-3601 *(Received: May 6, 1991; In Final Form: July 2, 1991)*

Formation of intramolecular triplet excimers in bridged diaryls is demonstrated for 2,2′-dinaphthylmethane (2,2′-DNM) and 2,2′-dinaphthyl ether (2,2′-DNE) using time-resolved absorption and emission (fluorescence and phosphorescence) spectroscopy. Comparison of the spectra of the ground-state dimer trapped in low-temperature glassy matrices with those of the molecules in fluid solution at room temperature suggests that the conformation of the intramolecular triplet excimers is similar to that of the corresponding ground-state-formed van der Waals dimers. Triplet–triplet annihilation of the excimer leading to the formation of the intramolecular excited singlet dimer at room temperature is also reported.

Introduction

Diaryl compounds have proven to be valuable systems in which to study the intermolecular interactions in the excited electronic state. It has been found that varying the distance which separates the two aromatic rings greatly affects the type of interaction between them. In the case of singlet excimers it has been demonstrated, through the study of 1,*n*-diphenyl-,[1] 1,*n*-dinaphthyl-,[2] 1,*n*-dipyrenyl-,[3] and 1,*n*-dicarbazolylalkanes,[4,5] that their formation is most favored when the two aromatic moieties are separated by four saturated bonds allowing the molecule to adopt a symmetrical sandwich configuration. When the linking chain is shorter than four bonds, it is impossible for the rings to attain the symmetric sandwich geometry[1-3] while for longer chains the probability to do so within the lifetime of the excited state decreases.[3] The stability of the sandwich-pair geometry of singlet-state excimers can be attributed to exciton resonance and charge resonance (the primary sources of the binding energy for singlet excimers), which are largest for the face-to-fact arrangement of the two aromatic rings.[6]

Substituted dinaphthylpropanes such as 1,3-bis(4-methoxy-1-naphthyl)propane and 1,3-bis(4-hydoxy-1-naphthyl)propane[7] exhibit, in addition to the monomer fluorescence and the normal excimer fluorescence, a second excimer emission located between the normal excimer and monomer fluorescence. This "second excimer" is characterized by a partial overlap between the two aromatic rings and is less stable than the normal singlet excimer with the sandwich configuration.

1,2-Di(*n*-anthryl)ethane,[8] a system where the two chromophores are separated by two saturated bonds, shows a broad structureless fluorescence in addition to the fluorescence from the locally excited (LE) state of anthracene. The broad emission has been ascribed to an intramolecular singlet excimer state with the two chromophores partially overlapped. The ratio of the quantum yield of the excimer fluorescence to that of the LE fluorescence yield was shown to increase with increasing solvent polarity, suggesting that the excimer state originates from an intramolecular charge transfer state.

In the extreme case of directly linked symmetric biaryls such as 9,9′-bianthryl[9] or 5,5′-bibenz[*a*]pyrenyl,[10] in which the formation of the sandwich type conformation is prohibited, the molecule is stabilized in the excited singlet state by assuming a minimum overlap configuration with the π-electron systems orthogonal to one another. This allows maximum charge separation

†On leave from the Institute of Physics PAN, Al. Lotnikow 32/46, 02-668 Warszawa, Poland.
‡The inaugural holder of the Goodyear Chair in Chemistry at The University of Akron.

(1) Hirayama, F. *J. Chem. Phys.* **1965**, *42*, 3163.
(2) Chandross, E.; Dempster, C. *J. Am. Chem. Soc.* **1970**, *92*, 3586.
(3) Zachariasse, K.; Kühnle, W. *Abstracts*, IUPAC Congress on Photochemistry, Enschede, 1974; p 197.
(4) Klöpffer, W. *Chem. Phys. Lett.* **1969**, *4*, 193.
(5) Masuhara, H.; Tamai, N.; Mataga, N.; De Schryver, F. C.; Vandendriessche, J. *J. Am. Chem. Soc.* **1983**, *105*, 7256.
(6) (a) Konijnenberg, E., Doctoral Thesis, Free University of Amsterdam, Holland, 1963. (b) Azumi, T.; Armstrong, A. T.; McGlynn, S. P. *J. Chem. Phys.* **1964**, *41*, 3839. (c) Vala, M. T.; Hiller, I. H.; Rice, S. A.; Jortner, J. *J. Chem. Phys.* **1966**, *44*, 23. (d) Murrell, J. N.; Tanaka, J. *J. Mol. Phys.* **1964**, *45*, 363. (e) Chandra, A. K.; Lim, E. C. *J. Chem. Phys.* **1968**, *49*, 5066.
(7) Itagaki, H.; Obukata, N.; Okamoto, A.; Horie, K.; Mita, I. *J. Am. Chem. Soc.* **1982**, *104*, 4469.
(8) (a) Hayashi, T.; Suzuki, T.; Mataga, N.; Sakata, Y.; Misumi, S. *J. Phys. Chem.* **1977**, *81*, 420. (b) Hayashi, T.; Mataga, N.; Umemoto, T.; Sakata, Y.; Misumi, S. *J. Phys. Chem.* **1977**, *81*, 424.
(9) Schneider, F.; Lippert, E. *Ber. Bunsenges. Phys. Chem.* **1970**, *72*, 624.
(10) Zander, M.; Rettig, W. *Chem. Phys. Lett.* **1984**, *110*, 602.

0022-3654/91/2095-9144$02.50/0